

The 1997 Umbria-Marche (central Italy) earthquake sequence: Insights on the mainshock ruptures from near source strong motion records

Aldo Zollo

Dipartimento di Scienze Fisiche, Università "Federico II", Napoli, Italy

Sandro Marcucci and Giuliano Milana

Servizio Sismico Nazionale, Roma, Italy

Paolo Capuano

Osservatorio Vesuviano, Napoli, Italy

Abstract. A small size foreshock and the two mainshocks of the Umbria Marche earthquake sequence which occurred on September 26, 1997 have been recorded by two digital 3C accelerometers located at near source distances. The close epicentral distance and azimuthal location relative to the fault orientation and geometry make these records relevant to look at the detail of the rupture kinematics. S-wave polarizations, apparent source time duration and waveforms from strong motion records are used to constrain the location of the fracture origin point, the fault geometry, the final slip distribution, size and mechanism of the events. The final model shows that the seismic ruptures occurred along two adjacent, sub-parallel, low angle dipping normal faults. The relative timing, location and geometry of the mainshock faults suggest the presence of a transfer zone (*barrier*) which has probably controlled the amplitude increase of local stress released by the first rupture at its NW edge which triggered about 9 hours later the second rupture.

Introduction

On September 26, 1997 two moderate size events ($M_W=5.7$ and $M_W=6.0$) stricken the Umbria-Marche region in Central Italy at 0033 and 0940 (GMT) producing few casualties and vast building damages. The two mainshocks occurred separated by 9 hours giving arise to an intense post-seismic activity lasting several months and characterized by hundreds of aftershocks including the sporadic occurrence of several magnitude 4.5-5.4 events. The fault plane solution for the two mainshocks have been evaluated by [Ekström *et al.*, 1998] applying the CMT technique on long period data. The results presented by these authors show, for both the events, a predominantly normal fault plane solution with strikes oriented in the Apennines direction (NNW-SSE). This normal faulting structure with extension perpendicular to the Apennine trend is consistent with the Quaternary tectonic of the internal sector

of the belt. In the region, the two main active normal faults bound Quaternary basins to the east [Cello *et al.*, 1997], whose extent are remarkable because they are linked to the size of fault fragments, showing permanent active deformation in the central Apennine [Meghraoui *et al.*, 1999]. Both CMT fault plane solutions and preliminary locations have been used as a starting point for the modeling proposed in this paper. In this study we used data collected by the only two digital strong motion instruments located at near source distances (within 30 km) from the epicenter of the events. In particular we used the near source accelerometric digital data recorded at Assisi (ASS) and Cerreto di Spoleto (TOR) (Figure 1) to investigate the details of the seismic source for the two mainshocks of the sequence. The close epicentral distance and azimuthal location relative to the presumed fault orientation and geometry make these records relevant to look at the detail of the rupture process. In order to account for all the problems related to seismic wave propagation we also applied the Empirical Green Function (EGF) technique obtaining the apparent source time function (STF) at the Assisi station. This was possible because the Assisi instrument recorded a foreshock [Amato *et al.*, 1998] of $M_W=4.5$ occurred on September 3 very close (Figure 1) to the September 26 events with a very similar S waves onset. The acceleration records have been band pass filtered in the range (1-5 Hz) and integrated to obtain the ground velocity.

Data modeling

In order to get a rough estimate of the source duration and spatial extension of the faulting phenomena, the Empirical Green Function method [Hartzell, 1978] was applied to estimate the apparent source time function for both the 0033 and 0940 events. The horizontal records of the foreshock event ($M_W=4.5$), which occurred on September 3, showing similar location and mechanism [Ekström *et al.*, 1998] have been used as EGF records. Unfortunately the only records at station Assisi could be used for this analysis. We used the deconvolution technique proposed by [Zollo *et al.*, 1995] which is based on the non linear inversion in the frequency range (0.1-10 Hz) of the strong motion records (S-wave window). The obtained solutions for

Copyright 1999 by the American Geophysical Union.

Paper number 1998GL005285.
0094-8276/99/1998GL005285\$05.00

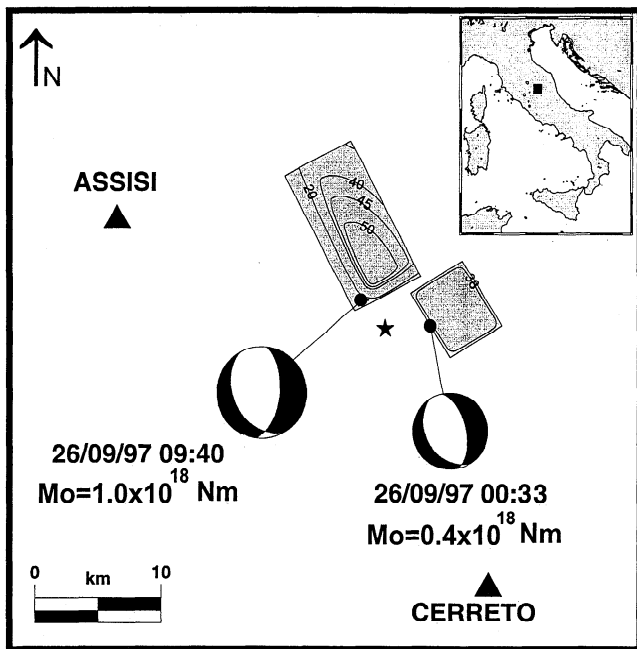


Figure 1. Sketch of the final rupture model for the 0033 and 0940 events. The black dots indicate the position of the rupture nucleation points on the fault planes. The black star indicate the foreshock location. Both the 0033 and 0940 rupture have been modeled using a constant rupture velocity (fault rupture parameters are given in Table 1). The final heterogeneous slip distribution for the 0940 event is shown on the fault plane (maximum about 55 cm). A homogeneous final slip model ($\langle \Delta u \rangle = 38$ cm) is obtained for the 0033 event.

the 0033 shock (Figure 2) shows two early prominent peaks shortly delayed (time difference: 0.7-0.8 s) and an approximate total duration of 2.5 s. The solution for the 0940 event shows a dominant initial peak and a rather constant behaviour of the STF with small amplitude fluctuations. The total duration of 0940 STF is estimated around 3 sec. We also computed a ratio of 2.6 between the integrals of the 0940 and 0033 STF's which is fairly consistent with the expected LP moment ratio between the two events (2.8-3.2), as computed by [Ekström *et al.*, 1998].

In the second step of our analysis we use the S polarization directions on filtered velocity records and the apparent source time duration at stations ASS and TOR to constrain the rupture nucleation point, the fault geometry and slip angles for both the events. An upper limit for the apparent source time duration at station TOR has been estimated on the horizontal acceleration records by measuring the time window which contained the maximum amplitude S-wave signals. In order to get the source mechanism and location parameters we used a grid search method by exploring the parameter space around the initial solution. The reference normal fault plane solutions are those computed by [Ekström *et al.*, 1998]. Based on early aftershock locations [Amato *et al.*, 1998] we selected the south-west dipping planes as the rupture surface. The method is based on the synthetic computation of maps of S-vector direction on the plane which presumably contain the fault

plane for a given fault mechanism solution (strike, dip, slip angle) and earthquake nucleation depth. Synthetic S-vector directions are computed at the earth surface by using the asymptotic Green's function for a double couple point-source model and assuming a 1-D layered velocity model. The best solution for fault mechanism angle and nucleation point location is chosen based on the misfit between observed and computed first S-polarization (Figure 3). The parameters obtained for the 0033 and the 0940 events are listed in Table 1. A preliminary estimate of the rupture length and width can also be inferred by plotting S-wave *isochrones* on the fault plane [Spudich and Frazer, 1984] and [Bernard and Madariaga, 1984] (Figure 3). For a given station the isochrone $t_D = T_S^o + \Delta t$ (T_S^o is the first S arrival time, Δt is the apparent source time duration) delimits the final rupture area as "seen" by this station according to a given value of rupture velocity. When the azimuthal location of stations around the fault plane is favourable the intersection area on the fault plane enclosed by all the isochrones t_D obtained for each station provide the best estimate of the final rupture surface, assuming a constant rupture velocity [Zollo and Bernard, 1991]. In the present case, although only two stations are available, they are located along nearly opposite directions relative to the expected fault geometry for both the 0033 and 0940 events. Plots of isochrones t_D for stations ASS and TOR for different rupture dimensions and velocities suggest for the 0940 event a final fault length of about 12 km, a width of about 7 km and a rupture propagating up-dip and NW from the rupture initiation point. Results of the similar analysis show that the 0033 event has an approximate size of 6×6 km² and that rupture propagated up-dip and SE of the nucleation point. The nucleation position for this event was further revised according to the waveform modeling which rather indicates an up-dip and bi-lateral propagation of the rupture. The isochrone plot for this event suggests that the second pulse on the apparent STF at station ASS (Figure 2) can be associated to the arrivals

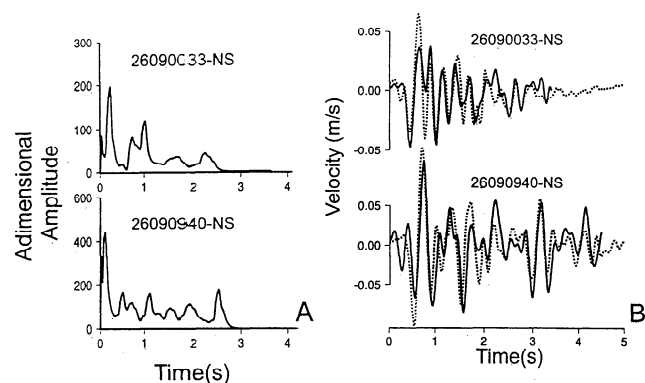


Figure 2. (A) Apparent source time functions at station ASS for the 0033 (top) and 0940 (bottom) events. The apparent STF's show an approximate total duration of 2.5s and 3s. The second pulse on apparent STF at ASS can be related to the arrival of strong stopping phases from the nearest northernmost fault border. (B) Comparison between mainshock (solid) and computed records velocity (dashed). The latter are obtained by direct convolution of apparent STF with the EGF records.

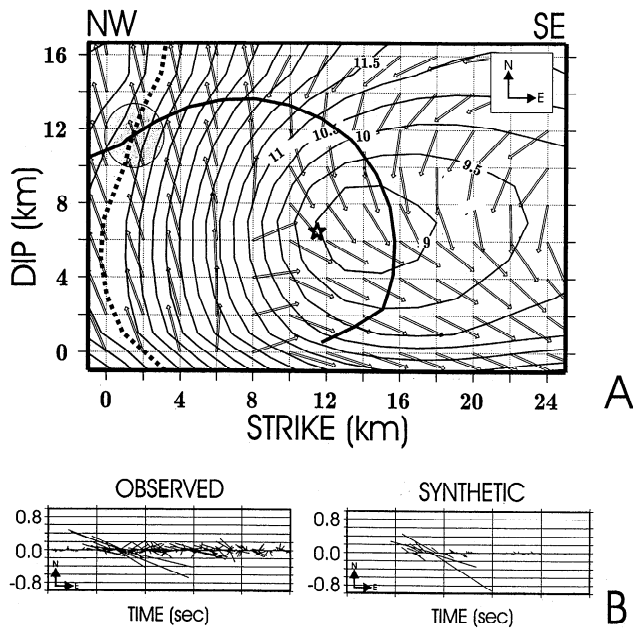


Figure 3. (A) Example of S-wave polarization analysis at station TOR for the 0940 event. Synthetic point source S vectors and isochrone contours are plotted on a plane containing the rupture plane; S vectors are represented in the N-E reference frame. Fault mechanism angles and rupture velocity are listed in Table 1. The asterisk shows the position on the fault of the rupture nucleation point. The solid thick and dotted curves indicate the isochrone t_D (see text) for stations ASS and TOR respectively. The shaded circle displays the intersection of t_D isochrones, which indicates the maximum rupture extent at NW. (B) Observed and synthetic S vector vs. time (polarigrams) for signals filtered in the frequency band 1-5 Hz are shown. The polarigrams display the S vector direction in the NE reference frame.

of stopping phases from the northernmost, nearest fault border (about 0.7-0.8 sec after the nucleation).

The final step of this analysis was the waveform modeling of ground velocity filtered in the 1-5 Hz frequency band. The method for computing synthetics is based on the computation of asymptotic Green's functions in a layered medium and the resolution of the source representation integral by a summation method along the isochrone, as proposed by [Bernard and Madariaga, 1984] and [Zollo and Bernard, 1991]. The slip rate function at each fault point is described by a box-car whose parameters are the rupture time, slip rate amplitude and duration. For our modeling we used a slip rate duration much smaller than the inverse of the higher frequency limit, which is equivalent to assume a delta-like slip rate function. We only considered the S-direct wave field, which is assumed to be dominant in near source records for the considered frequency and distance range. Anelastic attenuation is accounted for by convolution of the synthetic seismograms with the Azimi's function assuming a homogeneous $Q_S = 80$.

A trial and error approach was applied to model the NS and EW ground velocity records at stations ASS and TOR for the 0033 and 0940 events. The reference source parameters (location of the rupture nucleation

point, fault mechanism angles, length and width of the fault, rupture velocity and average slip) were inferred from previous analyses of source duration, S polarization and LP seismic moment estimates. Our trial and error waveform fitting started assuming homogeneous dislocation models and constant velocity rupture. More than 100 models have been checked varying the position of the nucleation point, fault mechanism angles, rupture velocity and slip distribution. Particularly for the 0940 event a heterogeneous slip rate distribution was needed to fit the waveforms and maximum amplitudes at the two stations (Figure 1). A homogeneous final slip model was instead sufficient to explain waveforms for the 0033 event (Figure 1 and Table 1). Comparison of observed and synthetic velocity records is shown in Figure 4.

Discussion and Conclusion

We modeled the two digital near source (within 30 km from the closest fault point) strong motion records (S-wave acceleration time series) of the Umbria Marche 1997 mainshocks. The inferred fault parameters for the 0033 and 0940 events are listed in Table 1 while a sketch of the rupture model is shown in Figure 1. For each event, we assumed a relatively simple rupture model with a single fault surface, homogeneous rupture velocity, rise time slip direction, and variable final slip distribution on the fault plane. The sensitivity of waveform misfit to changes of model parameters indicates that the parameter uncertainties are in the range 10%-20% of the values reported in Table 1. According to the results of this study the earthquakes are produced by two normal faulting ruptures having a small right lateral strike-slip component. The two faults have nearly the same strike (around 150° N) and dip (around 37°) angles. The two ruptures have nucleated from the fault bottom (8 km and 7 km for the 0033 and 0940, respectively) and show different directivity and rupture velocity. The 0033 event rupture propagated at an average speed of 3 km/s almost up-dip and bi-laterally, while the 0940 one moved at a slower speed (about 2.6 km/s) up-dip and North-West. The energetic arrival of stopping phases from the nearest, northernmost fault border can explain the second pulse of the 0033 apparent STF at station ASS. The two ruptures occurred on different length fault fragments (6 and 12 km respectively). A gaussian-like peak in the final slip distribu-

Table 1. Source parameters

Fault parameters	0033(GMT)	0940(GMT)
<i>strike</i>	148°	152°
<i>dip</i>	36°	38°
<i>slip</i>	-106°	-118°
M_0	$0.4 \times 10^{18} \text{ Nm}$	$1.0 \times 10^{18} \text{ Nm}$
L	$6 \times 10^3 \text{ m}$	$12 \times 10^3 \text{ m}$
W	$6 \times 10^3 \text{ m}$	$7.5 \times 10^3 \text{ m}$
$\langle \Delta u \rangle$	0.38 m	0.37 m
$\langle V_r \rangle$	$3 \times 10^3 \text{ m/s}$	$2.6 \times 10^3 \text{ m/s}$
$\langle \Delta \sigma \rangle$	1.9 MPa	1.5 MPa
<i>Bottom depth</i>	$7 \times 10^3 \text{ m}$	$8 \times 10^3 \text{ m}$

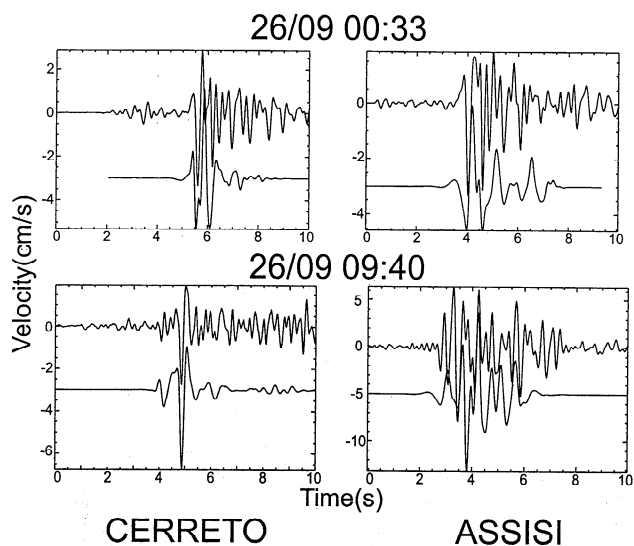


Figure 4. Comparison between observed (upper trace in each box) and synthetic velocity records of the two mainshocks, 0033 event (top) and 0940 event (bottom). Traces (NS component) are filtered in the 1-5 Hz frequency band. Amplitudes are in cm/sec.

tion is needed to model amplitudes and waveforms of the 0940 event. According to our simplified slip model the peak should be located at about 3-4 km up-dip and NW of the nucleation point (Figure 1). On the other hand a homogeneous ($\langle \Delta u \rangle = 0.38$ m) final slip model is able to describe the main waveform features for the 0033 event. Although the inferred maximum slip is rather different for the two events (about 38cm and 55cm) the average slip is nearly the same. The seismic moment difference appears therefore mainly controlled by the ruptured fault surface. The relative location and geometry of the faults indicates that they are low-angle, sub-parallel with a transfer zone having an approximate length of 5-7 km. This *barrier* has likely played a major role during the earthquake sequence by controlling the amplitude increase of local stress released by the 0033 rupture at its NW edge which triggered about 9 hours later the 0940 rupture. The inferred top of the faults for both the 0033 and 0940 is at about 3-3.5 km, according to our strong motion modeling. The depth range of the inferred fault zone appears consistent with the depth interval of aftershocks [Amato *et al.*, 1998]. Based on seismic reflection profiles in the area [Bally *et al.*, 1988] the low angle fault plane and normal faulting can be interpreted as inversion of pre-existing sub-parallel thrust fault fragments [Meghraoui *et al.*, 1999].

Acknowledgments. The authors thank the anonymous referee for constructive comments. A. Emolo, A. Herrero

and M. Meghraoui are thanked for their help and useful discussion. This research was supported by Murst 40% (1998) grant.

References

- Amato, A., R. Azzara, C. Chiarabba, G. B. Cimini, M. Cocco, M. Di Bona, L. Margheriti, S. Mazza, F. Mele, G. Selvaggi, A. Basili, E. Boschi, F. Courboulex, A. Deschamps, S. Gaffet, G. Bittarelli, L. Chiaraluce, D. Piccinini, and M. Ripepe, The 1997 Umbria-Marche, Italy, earthquake sequence: a first look at the main shocks and aftershocks, *Geophys. Res. Lett.*, **25**, 2861-2864, 1998.
- Bally, A.W., L. Burbi, J. Cooper, and R. Ghelardoni, Balanced sections and seismic reflection profiles across the central Apennines, *Mem. Soc. Geol. It.*, **35**, 257-310, 1988.
- Bernard, P., and R. Madariaga, A new asymptotic method for the modeling of near field accelerograms, *Bull. Seismol. Soc. Am.*, **74**, 539-559, 1984.
- Cello, G., S. Mazzoli, E. Tondi, and E. Turco, Active tectonics in the central Apennines and possible implications for seismic hazard analysis in peninsular Italy, *Tectonophysics* **272**, 43-68, 1997.
- Ekström, G., A. Morelli, E. Boschi, and A. M. Dziewonski, Moment tensor analysis of the central Italy earthquake sequence of September - October 1997, *Geophys. Res. Lett.*, **25**, 1971-1974, 1998.
- Hartzell, S., Earthquake aftershock as Green's functions, *Geophys. Res. Lett.*, **5**, 1-4, 1978.
- Meghraoui, M., V. Bosi, and T. Camelbeeck, Fault fragment control in the 1997 Umbria-Marche, central Italy, earthquake sequence, *Geophys. Res. Lett.*, **26**, 1069-1072, 1999.
- Spudich, P., and L. N. Frazer, Use of ray theory to calculate high frequency radiation from earthquake sources having spatially variable rupture velocity and stress drop, *Bull. Seismol. Soc. Am.*, **74**, 2061-2082, 1984.
- Zollo, A., P. Capuano, and S. K. Singh, Use of small earthquake record to determine source function of a larger earthquake: an alternative method and an application, *Bull. Seismol. Soc. Am.*, **85**, 1249-1256, 1995.
- Zollo, A., and P. Bernard, How does an asperity break? New elements from the waveform inversion of accelerograms for the 23:19, October 15, 1979 Imperial Valley aftershock, *J. Geophys. Res.*, **96**, 21549-21573, 1991.

A. Zollo, Dipartimento di Scienze Fisiche, Università "Federico II" Mostra d'Oltremare, 80125 Napoli, Italy.

(e-mail: aldo.zollo@na.infn.it)

S. Marucci and G. Milana, Servizio Sismico Nazionale, Via Curtatone 3, 00185 Roma, Italy.

(e-mail: milana@ssn.dstn.pcm.it)

P. Capuano, Osservatorio Vesuviano, Via Manzoni 249, 80123 Napoli, Italy. (e-mail: capuano@osve.unina.it)

(Received November 20, 1998; revised June 30, 1999; accepted July 22, 1999.)